Simon, Jonas; Schlapp-Hackl, Inge; Sapkota, Janak; Ristolainen, Matti; Rosenau, Thomas; Potthast, Antje

Towards Tailored Dialdehyde Cellulose Derivatives: A Strategy for Tuning the Glass Transition Temperature

Published in:
ChemSusChem

DOI:
10.1002/cssc.202300791

Published: 08/03/2024

Document Version
Publisher's PDF, also known as Version of record

Please cite the original version:
Simon, J., Schlapp-Hackl, I., Sapkota, J., Ristolainen, M., Rosenau, T., & Potthast, A. (2024). Towards Tailored Dialdehyde Cellulose Derivatives: A Strategy for Tuning the Glass Transition Temperature. *ChemSusChem*, *17*(5), Article e202300791. https://doi.org/10.1002/cssc.202300791

ChemSusChem
Research Article
doi.org/10.1002/cssc.202300791
Chemistry Europe
European Chemical Societies Publishing
www.chemsuschem.org

Towards Tailored Dialdehyde Cellulose Derivatives: A Strategy for Tuning the Glass Transition Temperature

Jonas Simon,[a] Inge Schlapp-Hackl,[b] Janak Sapkota,[c] Matti Ristolainen,[c]
Thomas Rosenau,*[a] and Antje Potthast*[a]

The derivatization of dialdehyde cellulose (DAC) has received increasing attention in the development of sustainable thermoplastics. In this study, a series of dialcohol celluloses were generated by borohydride reduction, which exhibited glass transition temperature (T_g) values ranging from 23 to 109 °C, depending on the initial degree of oxidation (DO) of the DAC intermediate. However, the DAC derivatives did not exhibit thermoplastic behavior when the DO of the modified DAC was below 26%. The influence of introduced side chains was highlighted by comparing DAC-based thermoplastic materials obtained by either oximation or borohydride reduction. Our results provide insights into the generation of DAC-based thermoplastics and highlight a strategy for tailoring the T_g by adjusting the DO during the periodate oxidation step and selecting appropriate substituents in subsequent modifications.

Introduction

Our society's use of fossil fuel-based plastics has led to disastrous global plastic pollution with detrimental consequences.[1] To deal with this problem and the depletion of fossil fuels,[2] the cellulose community has been working on developing alternative materials to replace petroleum-based thermoplastic products.[3]

The range of application for plastics is determined by their thermal properties, particularly their melting (T_m) or glass transition temperature (T_g).[4] Native cellulose cannot be reshaped into three-dimensional structures through heating alone. The energy required to break the interchain bonds[5,6] (specifically due to hydrogen bonding and some hydrophobic interactions) exceeds the degradation energy of cellulose. As a result, native cellulose degrades before undergoing any glass transition or melting event.[7,8]

One way to overcome this issue is by partially oxidizing cellulose with sodium periodate to generate dialdehyde cellulose (DAC). With the oxidant recycling issue having been solved[9] and a variety of subsequent modifications being at the chemists' disposal,[10] this approach appears to be both sustainable and quite versatile. Sodium periodate selectively cleaves the carbon-carbon bond between C2 and C3,[11,12] which – theoretically – should introduce increased flexibility to the polymer backbone and reduce the overall order and strength of hydrogen bonding. Both factors would favor the generation of thermoplastic materials from cellulose. However, the generated aldehyde groups in DAC are only partially present in the free form, while the majority crosslinks *in situ* to hemialdals and hemiacetals or form aldehyde hydrates (Scheme 1).[13–16] As a result, DAC is non-thermoplastic.[10] Further modification of the (masked) aldehyde groups, such as by borohydride reduction,[17–23] reductive amination,[10] or Passerini reaction,[24] reduces the strength of interchain interactions and eventually leads to cellulose-based thermoplastics.

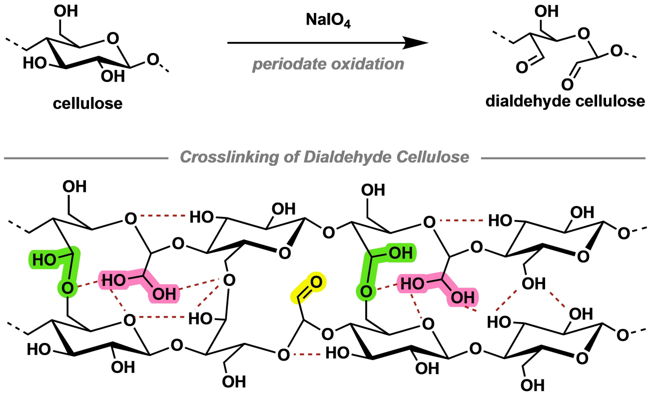

Scheme 1. Periodate oxidation of cellulose to generate dialdehyde cellulose (DAC; top) and the crosslinking behavior of the formally obtained aldehyde moiety by forming *in situ* hydrates, hemialdals and hemiacetals (bottom).

---

[a] *J. Simon, Prof. Dr. T. Rosenau, Prof. Dr. A. Potthast*
Department of Chemistry, Institute of Chemistry of Renewable Resources
University of Natural Resources and Life Sciences Vienna (BOKU)
Konrad-Lorenz-Strasse 24, 3430 Tulln (Austria)
E-mail: thomas.rosenau@boku.ac.at
antje.potthast@boku.ac.at

[b] *Dr. I. Schlapp-Hackl*
Department of Bioproducts and Biosystems
Aalto University
FI-00076 Aalto (Finland)

[c] *Dr. J. Sapkota, Dr. M. Ristolainen*
NE Research Center
UPM Pulp Research and Innovations
53200 Lappeenranta (Finland)

Supporting information for this article is available on the WWW under https://doi.org/10.1002/cssc.202300791

The dialcohol celluloses obtained by borohydride reduction of DAC showed T_g values above 75 °C.[17–21] Incomplete drying was found to decrease the T_g of dialcohol celluloses, likely due to the plasticizing effect of residual water molecules.[17,25] Additionally, the T_g shifted with the number of cleaved glucopyranose units – referred to as the degree of oxidation (DO).[17]

In a previous study, we introduced different primary amines into DAC with an initial DO of 39% through reductive amination.[10] The thermal properties of the resulting diamine celluloses were altered depending on the specific amine introduced, the obtained diamine celluloses having T_g values ranging from 71 to 112 °C. Furthermore, derivatization of water-soluble DAC with various isocyanides and carboxylic acids (Passerini reaction) was reported, yielding a series of DAC-based thermoplastics with very high T_g values (121–166 °C).[24] These recent studies have demonstrated that the T_g values of DAC-based thermoplastics are heavily influenced by both the backbone's flexibility and the chosen derivatization pathway.

Despite the successful generation of thermoplastics from DAC, questions remain about how to manipulate the flexibility of the backbone and the introduced side chains to control the T_g effectively. Additionally, it is unclear what DO is necessary to finally observe thermoplastic behavior after modification of the resulting DAC. The ability to tune T_g values in DAC-derivatives would be highly advantageous, as it would allow for precise manipulation of thermal properties to meet the specific requirements of different applications. For example, in their recent study, Larsson et al. produced injection molded caps from dialcohol cellulose.[22] In this context, the thermal properties must be competitive with PET's ($T_g = 76$ °C).[4,26] However, when it comes to applications for containers of hot beverages, a T_g value above 100 °C is essential for maintaining sufficient mechanical strength. Consequently, there is no such thing as a "good" or "bad" T_g; this depends on the respective application. Rather, the ability to tailor the T_g according to the target application is crucial when successful competition with commodity plastics is envisioned.

In addition to controlling the thermal properties, it is essential to consider other factors, such as minimizing chemical usage and resource consumption. Thus, synthetic approaches should favor the smallest degree of modification to reach the desired properties: therefore, it is crucial to know the smallest DO of DAC necessary to obtain DAC-based thermoplastics.

This study reports the synthesis of a series of thermoplastics from DAC. The overarching aims of the study were threefold: (A) To examine the effects of DO and introduced side groups on the T_g; (B) To evaluate which DO is required to generate DAC-based thermoplastics; and (C) to control the T_g within these limits. With this we hope to make a valuable contribution towards the production of sustainable thermoplastics from DAC with tailored thermal properties that can be optimized for the intended applications.

Results and Discussion

Effect of Backbone Flexibility

The rigidity of the polymer backbone in DAC derivatives can be controlled by adjusting the number of cleaved glucopyranose units through modulation of the DO. To investigate the effect of backbone flexibility on the T_g, we focused in the first part of this study on preparing a series of dialcohol celluloses by periodate oxidation/borohydride reduction of softwood kraft pulp (Figure 1A). After oxidizing softwood kraft pulp to produce a total of 26 DAC samples with degrees of oxidation ranging from 8 to 80%, the aldehyde groups were reduced using our previously reported borohydride reduction protocol[27] before being analyzed by DSC. The optimization toward effective conversion of the aldehyde groups, the characterization of the isolated dialcohol cellulose samples, as well as competing beta-elimination reactions have been reported in our previous work.[27]

Partial periodate oxidation introduces "soft" segments into the polymer backbone, which adds flexibility and reduces the strong interchain interactions in native cellulose (Figure 1B). The DSC data (Figure 1C) shows that the T_g of dialcohol cellulose is highly dependent on the initial DO of DAC, with T_g values ranging from 23 to 109 °C (Figure 1D; the entire DSC dataset is summarized in Table S3 and Figure S18). The T_g of amorphous and semi-crystalline polymers defines the temperature at which the polymer transitions from a defined shape to a viscous or rubbery state. At the molecular level, the T_g relates to the local relaxation of the polymer chains in amorphous, disordered regions. This energy highly depends on conformational barriers as well as intra- and intermolecular interactions.[4]

Thus, the T_g in dialcohol cellulose increased as the polymer chain becomes more rigid (with decreasing initial DO). The observed T_g values correlated linearly with the initial DO of the DAC-intermediate (Figure 1A).

A number of other influencing variables can explain minor deviations from the linear trend, as the T_g is influenced not only by polymer structure-property relationships. Crosslinking due to residual aldehyde groups was ruled out in our prior work by fluorescence labeling and GPC analysis.[27] Residual water in dialcohol celluloses has a plasticizing effect.[17,25] However, our DSC experiments involved a pre-drying step to ensure absence of residual water. The molecular weight of the polymer is another factor that can affect the T_g, particularly because it exponentially decreases in dialcohol cellulose with the initial DO.[27] Despite this, the isolated dialcohol celluloses were still high-molecular-weight polymers with M_w values above 30 kDa (Table S3), beyond which the effect of molecular weight on T_g becomes small according to the Flory-Fox equation.[28] Additionally, hemicelluloses and their conversion products may have a plasticizing effect. However, analysis of the molecular weight distributions of dialcohol celluloses indicates that any residual hemicelluloses were fully consumed during the periodate oxidation/borohydride reduction process and removed during the work-up procedure.[27] To further verify that hemicelluloses and their conversion products are not present and do not affect

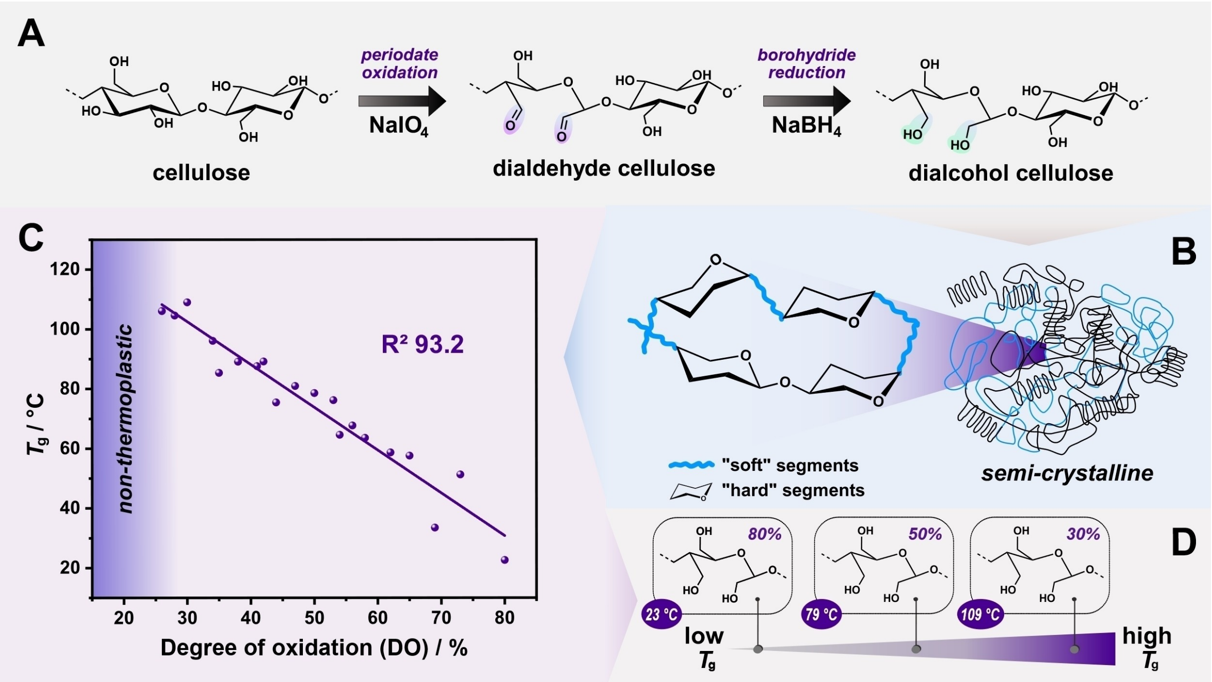

Figure 1. (A) Synthesis of dialcohol cellulose by periodate oxidation/borohydride reduction of cellulose *via* dialdehyde cellulose (DAC), (B) Illustration of the supramolecular structure of dialcohol cellulose containing both crystalline and amorphous regions (semi-crystalline), with a zoom into the polymer backbone composed of intact glucopyranose units ("hard" segments) and opened dialcohol cellulose units ("soft" segments), (C) Linear correlation between the obtained glass transition temperatures (T_g) of isolated dialcohol cellulose samples and the initial degree of oxidation (DO) of the DAC intermediate, (D) Illustration of the obtained glass transition temperatures, ranging from 23 to 109 °C, for the isolated dialcohol cellulose samples. The DO of the DAC intermediate is indicated.

the thermal data, we also examined a small series of dialcohol celluloses derived from "cotton linters" (Figure S20), which is a pure cellulose source without any hemicelluloses. The T_g values obtained from these samples were in a similar range to those derived from softwood kraft pulp.

The minor deviations in T_g from the linear trend are most likely caused by errors during DO determination of the DAC intermediate, as the determination of DO becomes less accurate for highly oxidized DAC samples due to over-oxidation phenomena and degradation reactions.[29] Additionally, beta-elimination reactions compete with borohydride reduction, leading to the generation of oligomers and low-molecular weight compounds[30–33] that potentially have a plasticizing effect on the isolated dialcohol celluloses, similar to the effect of residual water.

Analysis of the DSC data (Figure 1C) revealed that dialcohol celluloses from DAC with initial DO smaller than 26% showed no thermoplastic behavior. This phenomenon was also observed for a series of DAC-oximes, obtained from DAC and *O*-methylhydroxylamine hydrochloride (Figure S19). Notably, the dialcohol cellulose samples become non-thermoplastic well below their degradation temperature. However, it is challenging to determine the exact modification level required to generate DAC-based thermoplastics, as the transition is gradual. The DSC curves become more linear as the DO of the DAC intermediate decreases (Figure S18), making T_g determination increasingly difficult. White et al. established that polymers require a minimum free volume to enter a glassy state,[34] and it appears that dialcohol cellulose samples obtained from DAC with a DO below 26% did not reach this minimum free volume. This finding is supported by the observation that the DSC thermograms become more linear with decreasing DO. The crystallinity in dialcohol cellulose decreases with increasing degree of modification.[19] The polymer's crystallinity affects its mobility in amorphous regions, which leads to broadening of the glass transition.[35,36] At low degrees of oxidation, crystallinity and intermolecular forces are too pronounced and the chains still too confined that the free volume and a glassy state can be reached.

Effect of Side Chains

In addition to the ratio of cleaved and non-oxidized glucopyranose units in DAC derivatives, T_g can also be controlled by introducing different side chains along the cellulose backbone. To demonstrate the effect of these substituents, we reacted 39%-oxidized softwood kraft pulp with either sodium borohydride (reduction) or *O*-methylhydroxylamine hydrochloride or *O*-benzylhydroxylamine hydrochloride in an oximation (Figure 2A). The oximation reaction enables the introduction of various substituents into the "soft" segments of the polymer chains under mild conditions (Figure 2B). This enables the comparison of the influence of more sterically demanding substituents (which also have different polarity) in comparison to the hydroxy group (Figure 2C). *O*-methylhydroxylamine

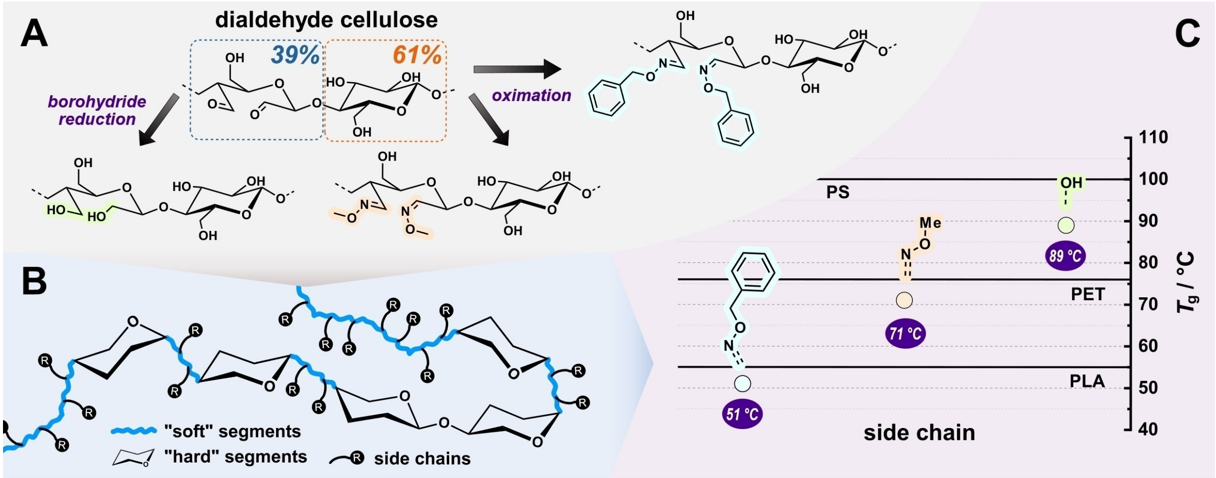

Figure 2. (A) Derivatization of 39 %-oxidized softwood kraft pulp by borohydride reduction and oximation reactions, (B) Illustration of the introduction of the side chains into the "soft" segments along the polymer backbone (hydroxy groups have been omitted to simplify), (C) Comparison of the determined glass transition temperatures (T_g) by differential scanning calorimetry (DSC) depending on the introduced substituent. The glass transition temperatures (T_g) of polystyrene (PS), polyethylene terephthalate (PET), and polylactic acid (PLA) are shown for comparison.

hydrochloride and *O*-benzylhydroxylamine hydrochloride are readily available commercially.

Both derivatization pathways (borohydride reduction and oximation) are known for their high conversion of the carbonyl groups in DAC (characterization of the isolated derivatives is summarized in the Supporting Information, Chapter 2). The NMR spectra of the DAC-oximes show a small formiate peak, indicative of the presence of residual aldehyde groups in the isolated materials.[31] In the case of dialcohol cellulose, some of the carbonyl groups also undergo beta-elimination.[27,30] However, the majority of aldehyde groups are converted to the corresponding alcohol or oxime derivative. The three DAC-based thermoplastics exhibited T_g values ranging from 51 to 89 °C (Figure 2C and Figure S21).

Dialcohol cellulose, which contains simple hydroxy groups along the polymer backbone, showed a remarkably higher T_g value (89 °C) compared to the two DAC-oximes from *O*-methylhydroxylamine (71 °C) and from *O*-benzylhydroxylamine (51 °C).

When side chains along the polymer backbone were introduced, the resulting change in T_g can be attributed to two opposing effects: (A) the introduction of substituents with conformational restriction that increase T_g, and (B) the addition of substituents that increase free volume and decrease T_g.[4] The hydroxy groups of dialcohol cellulose contribute very little to free volume. Replacing them with *O*-methyloxime groups added free volume without significantly increasing the conformational barrier, resulting in a slight decrease in T_g. This effect is even more pronounced when introducing the more bulky *O*-benzyloxime group, which adds substantially to free volume and leads to a significant decrease in T_g. Additionally, the hydroxy groups in dialcohol cellulose can participate in hydrogen bonding, resulting in increased interchain interactions and an increase in T_g compared to the oximes.

While it is possible to lower T_g even further by introducing bulky or long-chain substituents, such materials may not be suitable for many applications where high-T_g plastics are required. In such cases, it may be more useful to investigate the derivatization with compact substituents with high conformational barriers, such as aromatics, to increase the T_g. For example, in our previous study, we showed that by introducing aniline through reductive amination of 39 %-oxidized softwood kraft pulp the T_g increased to 112 °C.[10]

Effects of Cryo-Milling

The process of cryo-milling is anticipated to cause disorder in the polymer structure by means of shear stress. Since the T_g is affected by the crystallinity of the polymer, we hypothesized that cryo-milling might increase the molecular mobility by amorphization and therefore allow thermoplastic behavior even at lower degrees of modification.

Therefore, a series of dialcohol celluloses from DAC with varying DO (21, 23, 28 and 39 %) was cryo-milled for different time intervals (Figure 3A). Zhu et al. described the amorphization of PET by cryo-milling and quenching, however the observed transition temperatures (T_m and T_g) only slightly changed.[26] In our experiments, a substantial decrease in T_g was observed for the isolated dialcohol cellulose samples upon milling, reaching down to 42 °C (exemplarily shown in Figure 3C). This T_g shift became more prominent as the milling time increased, and the step height of the thermograms became more apparent (Figure S24). However, the Segal crystallinity index of the milled samples differs only slightly (Figure S27 and Table S4) and therefore the change in T_g cannot be attributed to crystallinity loss (the transition from crystalline to amorphous regions).

In the case of never-dried dialcohol cellulose from DAC (with an initial DO of 21 %), GPC analysis was performed, which revealed progressive degradation of the polymer chains with increasing milling time (Figure 3B). This behavior is also known for genuine, non-modified cellulose.[37,38] Consequently, it is

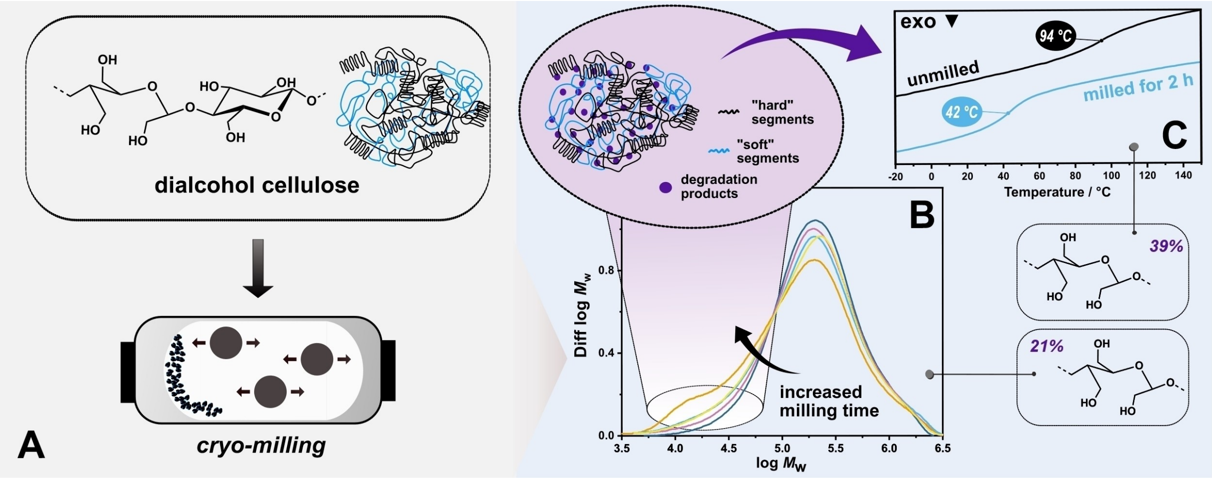

Figure 3. (A) Illustration of the cryo-milling process of dialcohol cellulose, (B) Illustration of the changes in the molecular weight distributions of dialcohol cellulose (initial degree of oxidation: 21 %) depending on the milling time. The low-molecular-weight fraction after cryo-milling can be attributed to oligomers formed due to degradation processes. (C) DSC thermograms of dialcohol cellulose (initial degree of oxidation: 39 %) without milling and after cryo-milling for two hours. The glass transition temperature (T_g) decreased significantly from 94 to 42 °C as a consequence of the milling.

highly probable that the degradation products act as plasticizers, similar to the effect of residual water.[17] No T_g was observed for dialcohol cellulose derived from DAC with an initial DO of 21 % and cryo-milling did not significantly reduce the modification threshold required to produce DAC-based thermoplastics. However, it is important to note that the glass transitions in the thermograms became more profound for dialcohol cellulose samples that were close to the threshold (as shown in Figure S24 and S25) of being thermoplastic. This effect was also observed for dialcohol cellulose with an initial DO of 23 % for the DAC-intermediate, where no T_g was observed prior to milling (at least it was not discernible in the DSC thermogram). The plasticizing effect of degradation products is also important when considering work-up protocols and purification of the polymers. Inadequate purification which fails to remove low-molecular weight degradation products is likely to result in a decreased $T_{g.}$

Conclusions

DAC, obtained from periodate oxidation of cellulosic substrates, can readily be converted into sustainable thermoplastics through further derivatization. This study demonstrated the T_g of these thermoplastics to be easily controllable by adjusting the DO and this way the ratio of modified and non-oxidized glucopyranose units. A series of DAC-based thermoplastics was generated by oximation reactions and borohydride reductions. Upon borohydride reduction of DAC, the isolated dialcohol celluloses exhibited T_g values ranging from 23 to 109 °C – just by adjusting the initial DO during periodate oxidation. The DAC-derivatives exhibited no thermoplastic behavior when the DO of the modified DAC was below 26 %.

It was expected that cryo-milling would in general enhance the overall molecular mobility of DAC-derivatives. Still, it did not facilitate the generation of thermoplastic dialcohol celluloses from DAC when the initial DO was below 26 %. Nevertheless, the T_g of dialcohol celluloses with higher degrees of modification was lowered significantly with increasing milling time due to the formation of degradation products, which acted as plasticizers.

In addition to adjusting the DO of DAC, the T_g was significantly affected by the introduced side chains along the polymer backbone. From comparing the DSC thermograms of a series of oximes and dialcohol celluloses, it was evident that the T_g decreased with increasing free volume caused by bulky substituents, while it increased with increasing interchain interactions. The T_g of dialcohol cellulose showed the highest value of the entire series (89 °C).

With this work, we presented a strategy to tailor the thermoplastic behavior in DAC-derivatives by either setting the initial DO of the DAC intermediate or (B) selecting appropriate substituents for a subsequent derivatization. Either of these approaches enables the creation of thermoplastic materials from DAC. For packaging applications, T_g values around 100 °C, similar to those of PS (100 °C)[39] or PET (76 °C),[26] are desirable, whereas for drug delivery systems, lower T_g values are typically preferred. In terms of the achievable T_g values, the DAC derivatives presented would be suitable for both of these application fields.

Follow-up chemistry should prioritize minimum degrees of modification to generate the desired thermal properties to save resources and chemicals during periodate oxidation and subsequent modification. Despite that, it is evident that derivatization pathways which make use of non-toxic substituents are to be favored.

Experimental Section

Chemicals and Reagents

Softwood kraft pulp (mix of spruce and pine) was provided by UPM-Kymmene Oyj (Lappeenranta, Finland). The hemicellulose content of the pulp was determined to be 8.5% by analyzing the C4 resonance from the ^{13}C solid-state NMR spectrum according to Jusner et al. (Figure S4 and Table S1).[40] The deconvolution data were consistent with results obtained from monosaccharide quantification, according to Sundberg et al. (Table S2).[41] The softwood kraft pulp was previously characterized by GPC-MALLS (M_n = 55 kDa, M_w = 614 kDa, M_z = 1651 kDa, and $Đ$ = 11.1; Figure S1) and disintegrated in deionized water before use with a commercial kitchen blender. Sodium periodate (≥99.8%; Sigma Aldrich), hydroxylamine hydrochloride (99%; Sigma-Aldrich), sodium borohydride (≥98.0%; Sigma-Aldrich), *O*-methylhydroxyl-amine hydrochloride (98%; Sigma-Aldrich), *O*-benzylhydroxyl-amine hydrochloride (99%; Sigma Aldrich), citric acid monohydrate (≥ 99%; Fisher Chemical), and sodium phosphate monobasic monohydrate (≥99.0%; Sigma-Aldrich) were without further purification.

Characterization

Gel permeation chromatography (GPC) was performed using the following size exclusion/multiangle light scattering (SEC-MALLS) system: MALLS detector (Wyatt Dawn DSP, Wyatt Inc.), refractive index detector (Shodex RI-71, Showa Denko K.K.), four Waters HPLC columns (Styrage HMW 6E, 7.8×300 mm, 15–20 μm), Agilent GPC/SEC guard column (PL gel mixed ALS, 7.8×50 mm, 20 μm), Bio-Inert 1260 Infinity II pump (Agilent), and autosampler (HP Series 1100, Agilent). The mobile phase was *N*,*N*-dimethylacetamide/lithium chloride (0.9% w/v; filtered through a 0.02 μm filter), and 100 μL of each sample was injected with a 45-minute run time at a flow rate of 1 mL/min. All GPC samples were first dissolved in *N*,*N*-dimethylacetamide/lithium chloride (9% w/v) and then filtered through a 0.45 μm syringe filter following the standard protocol.[42] The molecular weight distributions and the GPC–MALLS statistical moments were calculated based on a refractive index increment of 0.140 mL/g for cellulose in *N*,*N*-dimethylacetamide/lithium chloride (0.9% w/v) at 488 nm. The raw data were processed with Astra 4.7 and GRAMS/AI 7.0 software.

Differential scanning calorimetry (DSC) thermograms were measured under nitrogen (250 mL/min) on a DSC 214 Polyma (NETZSCH). About 7–10 mg of each freeze-dried sample was weighed, added to a pierced aluminum crucible, heated, and held at 100 °C for 20 minutes. After drying, the sample was passed through a heat–cool–heat cycle at 10 °C/min. The temperature ranged from −50 (min) to 180 °C (max), and the reported data are from the second heating cycle. NETZSCH's spectroscopy software Proteus® (v 8.0.2) was used for processing DSC data.

Fourier-transform infrared (FTIR) spectroscopy was conducted using a Frontier FTIR spectrophotometer (PerkinElmer) operating in attenuated total reflection (ATR) mode. All samples were air-dried for 3 to 5 days and conditioned in the measuring room before analysis. Spectra were recorded by accumulation of 32 scans per sample at a resolution of 4 cm^{-1} over the range of 4000–600 cm^{-1}.

All NMR spectra were recorded on a Bruker Avance II 400 spectrometer at room temperature. The NMR spectra of dialcohol cellulose were measured at elevated temperature (333 K). The materials were characterized by ^{1}H, HSQC and HMBC experiments. All NMR samples were prepared according to published protocols in a [P_{4444}][OAc]:DMSO-d_6 (1:4 wt%) electrolyte (Cellolyte obtained from Innotope).[43–45] Chemical shifts are reported in parts per million (ppm) downfield relative to the residual proton of DMSO-d_6.

Carbon (^{13}C) cross polarization/magic angle spinning (CP/MAS) NMR spectra were recorded on a Bruker Avance III HD 400 spectrometer with a resonance frequency of 400.34 MHz and 100.67 MHz for ^{1}H and ^{13}C, respectively, equipped with a 4 mm dual broadband CP/MAS probe. Data were acquired at a spinning rate of 12 kHz, with a CP contact time of 2 ms and SPINAL 64 ^{1}H decoupling. Chemical shifts were referenced externally against the carbonyl signal of glycine with $\delta = 176.03$ ppm. Deconvolution of the C4 resonance (91–79 ppm) was carried out according to Jusner et al.[40]

X-ray diffraction patterns were recorded on a Xenocs Xeuss 3.0 X-ray diffractometer operated in transmission mode using CuKα radiation ($\lambda = 1.54189$ Å) at 50 kV/0.6 mA equipped with a Dectris Eiger2 R 1 M detector. The segal crystallinity index (segal CI) was calculated according to Nam et al.[46]

Synthesis of Dialdehyde Cellulose

Periodate oxidation of softwood kraft pulp was performed according to our previously reported protocol.[47] Briefly, disintegrated softwood kraft pulp was added to deionized water and sodium periodate. The reaction mixture was stirred in the dark to limit photochemical side reactions. The DO was controlled by adjusting the temperature, periodate concentration, and reaction time. The resulting dialdehyde celluloses were filtered off and thoroughly washed with deionized water. Gel-like DAC samples were further treated with a sodium thiosulfate solution to deactivate oxidizing iodine species. All samples were then stored in a never-dried state at −20 °C until further characterization or derivatization.

Borohydride Reduction of Dialdehyde Cellulose

Borohydride reduction was performed according to our standard procedure reported previously.[27] Briefly, in a 100 mL round-bottom flask, sodium borohydride (5 equiv. based on the carbonyl groups in DAC) and aqueous monobasic sodium phosphate solution (50 mL) were added. The concentration of monobasic sodium phosphate was adjusted to set a pH of 10 at the start of the reduction. To this mixture, 400 mg DAC (on a dry basis; 1 equiv.) was added, the reaction mixture was stirred for 140 minutes at 45 °C, and the reaction terminated with acetic acid. Dialcohol celluloses from highly oxidized DAC became (partially) soluble in water and were subsequently precipitated in cold methanol and isolated by centrifugation. The crude products were washed with deionized water and ethanol, whereas the water-soluble dialcohol celluloses were washed with cold methanol. All samples were freeze-dried and analyzed by DSC.

Oximation of Dialdehyde Cellulose

In a 50 mL round-bottom flask, *O*-methylhydroxylamine hydrochloride or *O*-benzylhydroxyl-amine hydrochloride (5 equiv. based on the carbonyl groups in DAC) was dissolved in citric acid-sodium phosphate buffer (50 mL, pH 5.0). DAC (200 mg, on a dry basis; 1 equiv.) was added, and the reaction mixture was stirred at room temperature for 20 hours. The resulting oximes were precipitated in cold methanol and isolated by centrifugation. The crude products were then washed with cold methanol and stored in a never-dried state at -20 °C until further characterization.

Determination of the Degree of Oxidation

The DO of DAC was determined from the FTIR spectra using the previously published partial least square regression model.[16,48]

Cryo-milling Experiments

Dialcohol cellulose samples with varying degrees of oxidation were cryomilled using a vibrational mill (Retsch CryoMill, Retsch GmbH). Approximately 100 mg of the freeze-dried sample was placed in a grinding jar (coated with polytetrafluoroethylene) containing three grinding balls and then milled at a frequency of 25 s^{-1} for various time intervals. To maintain a low temperature throughout the milling process, liquid nitrogen was continuously introduced into the outer vial of the grinding jar. The process was repeated using dialcohol cellulose (DO of 21%) in a never-dried state and with a larger sample size.

Acknowledgements

We kindly thank Business Finland and UPM-Kymmene Oyj (Finland) for their financial support and gratefully acknowledge the support by the BOKU doctoral school ABC&M and the Austrian Biorefinery Center Tulln (ABCT). We also thank Dr. Markus Bacher for his help with the NMR measurements.

Conflict of Interests

The authors declare no conflict of interest.

Data Availability Statement

Additional data that support the findings of this study are available from the corresponding author upon request.

Keywords: glass transition temperature · material science · periodate oxidation · renewable resources · thermoplastic polymers

[1] M. Matthew, A. H. P. H, T. M. B, J. Annika, *Science (1979)* **2021**, *373*, 61–65.
[2] S. Shafiee, E. Topal, *Energy Policy* **2009**, *37*, 181–189.
[3] G. Dalei, S. Das, M. Pradhan, *Cellulose* **2022**, *29*, 1–33.
[4] H. T. H. Nguyen, P. Qi, M. Rostagno, A. Feteha, S. A. Miller, *J. Mater. Chem. A* **2018**, *6*, 9298–9331.
[5] K. Mazeau, L. Heux, *J. Phys. Chem. B* **2003**, *107*, 2394–2403.
[6] W. G. Glasser, R. H. Atalla, J. Blackwell, R. Malcolm Brown, W. Burchard, A. D. French, D. O. Klemm, Y. Nishiyama, *Cellulose* **2012**, *19*, 589–598.
[7] L. Szcześniak, A. Rachocki, J. Tritt-Goc, *Cellulose* **2008**, *15*, 445–451.
[8] C. Li, J. Wu, H. Shi, Z. Xia, J. K. Sahoo, J. Yeo, D. L. Kaplan, *Adv. Mater.* **2022**, *34*, 2105196.
[9] S. Koprivica, M. Siller, T. Hosoya, W. Roggenstein, T. Rosenau, A. Potthast, *ChemSusChem* **2016**, *9*, 825–833.
[10] J. Simon, L. Fliri, J. Sapkota, M. Ristolainen, A. S. Miller, M. Hummel, T. Rosenau, A. Potthast, *Biomacromolecules* **2023**, *24*, 166–177.
[11] E. L. Jackson, C. S. Hudson, *J. Am. Chem. Soc.* **1937**, *59*, 2049–2050.
[12] T. Nypelö, B. Berke, S. Spirk, J. A. Sirviö, *Carbohydr. Polym.* **2021**, *252*, 117105.
[13] H. Amer, T. Nypelö, I. Sulaeva, M. Bacher, U. Henniges, A. Potthast, T. Rosenau, *Biomacromolecules* **2016**, *17*, 2972–2980.
[14] U.-J. Kim, S. Kuga, M. Wada, T. Okano, T. Kondo, *Biomacromolecules* **2000**, *1*, 488–492.
[15] H. Spedding, *J. Chem. Soc. (Resumed)* **1960**, 3147–3152.
[16] J. Simon, O. Tsetsgee, N. A. Iqbal, J. Sapkota, M. Ristolainen, T. Rosenau, A. Potthast, *Carbohydr. Polym.* **2022**, *278*, 118887.
[17] W. Kasai, T. Morooka, M. Ek, *Cellulose* **2014**, *21*, 769–776.
[18] P. A. Larsson, L. A. Berglund, L. Wågberg, *Biomacromolecules* **2014**, *15*, 2218–2223.
[19] P. A. Larsson, L. A. Berglund, L. Wågberg, *Cellulose* **2014**, *21*, 323–333.
[20] V. López Durán, P. A. Larsson, L. Wågberg, *Cellulose* **2016**, *23*, 3495–3510.
[21] B. Lei, Y. Feng, *J. Cleaner Prod.* **2020**, *265*, 121631.
[22] G. Lo Re, E. R. Engel, L. Björn, M. G. Sicairos, M. Liebi, J. Wahlberg, K. Jonasson, P. A. Larsson, *Chem. Eng. J.* **2023**, *458*, 141372.
[23] E. Linvill, P. A. Larsson, S. Östlund, *Mater. Des.* **2017**, *128*, 231–240.
[24] E. Esen, M. A. R. Meier, *ACS Sustainable Chem. Eng.* **2020**, *8*, 15755–15760.
[25] A. Y. Mehandzhiyski, E. Engel, P. A. Larsson, G. Lo Re, I. V. Zozoulenko, *ACS Appl. Bio. Mater.* **2022**, *5*, 4793–4802.
[26] Y. G. Zhu, Z. Q. Li, D. Zhang, T. Tanimoto, *J. Appl. Polym. Sci.* **2006**, *99*, 2868–2873.
[27] J. Simon, L. Fliri, F. Fröhlich, J. Sapkota, M. Ristolainen, M. Hummel, T. Rosenau, A. Potthast, *Cellulose* **2023**, *30*, 8205–8220.
[28] T. G. Fox, P. J. Flory, *J. Appl. Phys.* **1950**, *21*, 581–591.
[29] J. Leguy, Y. Nishiyama, B. Jean, L. Heux, *ACS Sustainable Chem. Eng.* **2019**, *7*, 412–420.
[30] A. Potthast, S. Schiehser, T. Rosenau, M. Kostic, *Holzforschung* **2009**, *63*, 12–17.
[31] P. Liu, B. Pang, S. Dechert, X. C. Zhang, L. B. Andreas, S. Fischer, F. Meyer, K. Zhang, *Angew. Chem. Int. Ed.* **2020**, *59*, 3218–3225.
[32] T. Hosoya, M. Bacher, A. Potthast, T. Elder, T. Rosenau, *Cellulose* **2018**, *25*, 3797–3814.
[33] C.-Q. Ruan, M. Strømme, J. Lindh, *Carbohydr. Polym.* **2018**, *181*, 200–207.
[34] R. P. White, J. E. G. Lipson, *Macromolecules* **2016**, *49*, 3987–4007.
[35] N. M. Alves, J. F. Mano, E. Balaguer, J. M. M. Dueñas, J. L. G. Ribelles, *Polymer (Guildf)* **2002**, *43*, 4111–4122.
[36] J. H. Griffith, B. G. Rånby, *J. Polym. Sci.* **1960**, *44*, 369–381.
[37] I. Solala, U. Henniges, K. F. Pirker, T. Rosenau, A. Potthast, T. Vuorinen, *Cellulose* **2015**, *22*, 3217–3224.
[38] Z. Ling, T. Wang, M. Makarem, M. Santiago Cintrón, H. N. Cheng, X. Kang, M. Bacher, A. Potthast, T. Rosenau, H. King, *Cellulose* **2019**, *26*, 305–328.
[39] J. Rieger, *J. Therm. Anal.* **1996**, *46*, 965–972.
[40] P. Jusner, M. Bacher, J. Simon, F. Bausch, H. Khaliliyan, S. Schiehser, I. Sumerskii, E. Schwaiger, A. Potthast, T. Rosenau, *Cellulose* **2022**, *29*, 1081–1095.
[41] A. Sundberg, K. Sundberg, C. Lillandt, B. Holmhom, *Nord. Pulp Pap. Res. J.* **1996**, *11*, 216–219.
[42] A. Potthast, S. Radosta, B. Saake, S. Lebioda, T. Heinze, U. Henniges, A. Isogai, A. Koschella, P. Kosma, T. Rosenau, *Cellulose* **2015**, *22*, 1591–1613.
[43] L. Fliri, K. Heise, T. Koso, A. R. Todorov, D. R. del Cerro, S. Hietala, J. Fiskari, I. Kilpeläinen, M. Hummel, A. W. T. King, *Nat. Protoc.* **2023**, *18*, 2084–2123.
[44] A. W. T. King, V. Mäkelä, S. A. Kedzior, T. Laaksonen, G. J. Partl, S. Heikkinen, H. Koskela, H. A. Heikkinen, A. J. Holding, E. D. Cranston, I. Kilpeläinen, *Biomacromolecules* **2018**, *19*, 2708–2720.
[45] T. Koso, D. Rico del Cerro, S. Heikkinen, T. Nypelö, J. Buffiere, J. E. Perea-Buceta, A. Potthast, T. Rosenau, H. Heikkinen, H. Maaheimo, A. Isogai, I. Kilpeläinen, A. W. T. King, *Cellulose* **2020**, *27*, 7929–7953.
[46] S. Nam, A. D. French, B. D. Condon, M. Concha, *Carbohydr. Polym.* **2016**, *135*, 1–9.
[47] J. Simon, L. Fliri, F. Drexler, M. Bacher, J. Sapkota, M. Ristolainen, M. Hummel, A. Potthast, T. Rosenau, *Carbohydr. Polym.* **2023**, *310*, 120691.
[48] J. Simon, O. Tsetsgee, N. A. Iqbal, J. Sapkota, M. Ristolainen, T. Rosenau, A. Potthast, *Data Brief* **2021**, *40*, 107757.

Manuscript received: June 27, 2023
Revised manuscript received: November 3, 2023
Accepted manuscript online: November 3, 2023
Version of record online: November 17, 2023